



Investigation on the role of the tetrazole in the binding of thiotetrazolylacetanilides with HIV-1 wild type and K103N/Y181C double mutant reverse transcriptases

Alexandre Gagnon*, Serge Landry, René Coulombe, Araz Jakalian, Ingrid Guse, Bounkham Thavonekham, Pierre R. Bonneau, Christiane Yoakim, Bruno Simoneau

Boehringer Ingelheim (Canada) Ltd., Research and Development, 2100 Cunard Street, Laval, Que., Canada H7S 2G5

ARTICLE INFO

Article history:

Received 18 November 2008
Revised 17 December 2008
Accepted 17 December 2008
Available online 24 December 2008

Keywords:

Non-nucleoside reverse transcriptase inhibitors (NNRTIs)
Thiotetrazoles
Electrostatic potential
Molecular modeling
Double mutant reverse transcriptase

ABSTRACT

The role of the tetrazole moiety in the binding of aryl thiotetrazolylacetanilides with HIV-1 wild type and K103N/Y181C double mutant reverse transcriptases was explored. Different acyclic, cyclic and heterocyclic replacements were investigated in order to evaluate the conformational and electronic contribution of the tetrazole ring to the binding of the inhibitors in the NNRTI pocket. The replacement of the tetrazole by a pyrazolyl group led to reversal of selectivity, providing inhibitors with excellent potency against the double mutant reverse transcriptase.

© 2008 Elsevier Ltd. All rights reserved.

According to the world health organization, every day, more than 6800 people become infected with human immunodeficiency virus (HIV) and over 5700 people die from acquired immunodeficiency syndrome (AIDS) throughout the world.¹ With an estimated number of 33.2 million people living with AIDS in 2007, an adequate access to HIV treatment remains critical. Twelve years after the introduction of highly active antiretroviral therapy (HAART) for the treatment of HIV, the development of potent and well tolerated new drugs remains an active field of research.² The HIV reverse transcriptase (RT) enzyme plays an essential role in the replication of the HIV virus by performing the retrotranscription of the viral RNA into viral DNA. Therefore, the HIV-RT constitutes a major target for antiretroviral drug development.³ The non-nucleoside reverse transcriptase inhibitors (NNRTIs) interact in an allosteric site located approximately 10 Å away from the catalytic site, causing enzyme inhibition.⁴ Although NNRTIs are commonly used in HAART regimens, the low genetic barrier to mutation associated with first line NNRTIs creates a need for new drugs that exhibit activity against the most prevalent mutants.⁵

We⁶ and others⁷ have recently reported the discovery of aryl-thiotetrazolyl acetanilide **1** (Fig. 1) as a low nanomolar inhibitor of the wild type (WT) HIV-1 RT. More importantly, compound **1**,

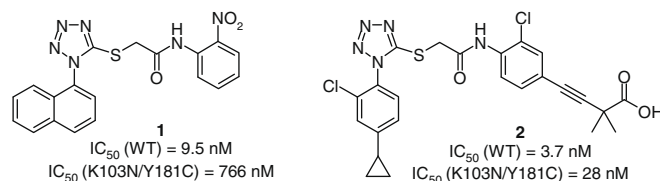


Figure 1. Hit compound **1** and optimized inhibitor **2** obtained following uHTS campaign and lead optimization program.

which was identified in the course of a ultra high-throughput screening (uHTS) campaign, also showed submicromolar potency against the clinically relevant K103N/Y181C double mutant (DM) RT.⁸ Excellent potency against this mutant is highly desirable for second generation drugs since it plays a central role in the development of resistance in patients exposed to nevirapine, efavirenz and delavirdine.⁹ An intensive lead optimization program subsequently led to the design of compound **2** which possesses key features that provide optimal binding to the reverse transcriptase, such as a 2,4-disubstituted left hand side aryl group and a 2-chloro-4-alkynyl anilide right hand side fragment.¹⁰ We recently disclosed the detailed SAR studies of the alkyne series¹¹ and showed that compound **2** gives good cellular potency against the WT and the K103N/Y181C DM RT in combination with good pharmacokinetic parameters in rats.

* Corresponding author. Tel.: +1 450 682 4640; fax: +1 514 682 4189.
E-mail address: alexandre.gagnon@boehringer-ingelheim.com (A. Gagnon).

Previous studies conducted by us on the tetrazolyl inhibitors bound in the WT NNRTI pocket suggested that the tetrazolyl group is likely involved in relatively weak associations with the side chains of Y181 and/or K103.¹² Consequently, we proposed at that time that this heterocycle is more than simply a scaffold that orients the pharmacophores in the optimal geometry. In order to have a better understanding of the role of this group in the binding of the inhibitors with the RT enzyme, we initiated SAR studies centered around this area of the molecule. As a first step toward this goal, we recently reported that amides, carbamates, ureas and thioamides **3** efficiently behave as tetrazole replacements (Fig. 2).¹² Additionally, others have reported that analogs of **4** provide excellent potency against the WT and the K103N/Y181C RT, showing that the triazole is also a good tetrazole surrogate.¹³ Recently, thiadiazoles **5**, which we first reported in 2005,¹⁰ were also shown to be adequate tetrazole replacements.¹⁴

We would like to report herein our studies in the evaluation of the electronic and conformational contribution of the tetrazolyl group to the binding of the inhibitors with the HIV-1 RT. Taking lessons from series **3**, **4** and **5** we set for ourselves the objective of finding a rigidified linker that would provide the optimal binding conformation in conjunction with the required electronic fingerprint (Fig. 3). Knowing from previous modeling studies that the tetrazole is in the vicinity of residue 103,^{11,12} we utilized the clinically relevant K103N/Y181C double mutant RT as a probe to gain insights into the nature and strength of the interactions between the linker and the protein.

We initiated our studies by exploring the conformational role of the tetrazolyl group (Table 1) through the use of simple all-carbon cyclic and acyclic linkers. In the event, replacing the tetrazolyl group in **6** with a *Z* alkene (compound **8**) resulted in a 7-fold reduction of potency against the WT-RT, showing that a simple double bond is capable of partially retaining the potency against the WT-RT. However, a drastic decrease of activity against the DM-RT was observed. Surprisingly, the *E* alkene **9** retained submicromolar potency against the WT-RT, but led to poor activity against the DM-RT. These isomeric alkenes clearly demonstrate a preference for a *cis* geometry, supporting the hypothesis that the tetrazole partially acts as an orienting scaffold. Using compound **7** as a ref-

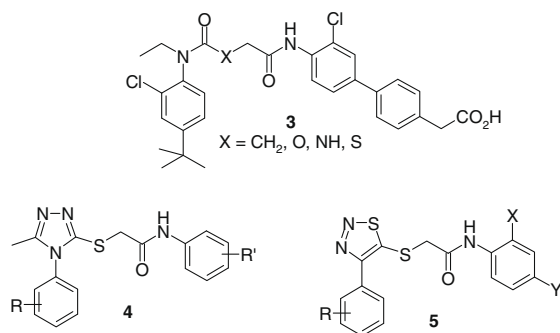


Figure 2. Amides, carbamates, ureas, thiocarbamates **3**, triazoles **4** and thiadiazoles **5** as potent inhibitors of the HIV-1 wild type and K103N/Y181C double mutant reverse transcriptases.

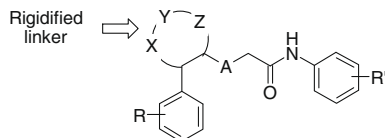


Figure 3. Design of a conformationally constrained linker acting as a tetrazole replacement.

Table 1
Evaluation of cyclic and acyclic linkers

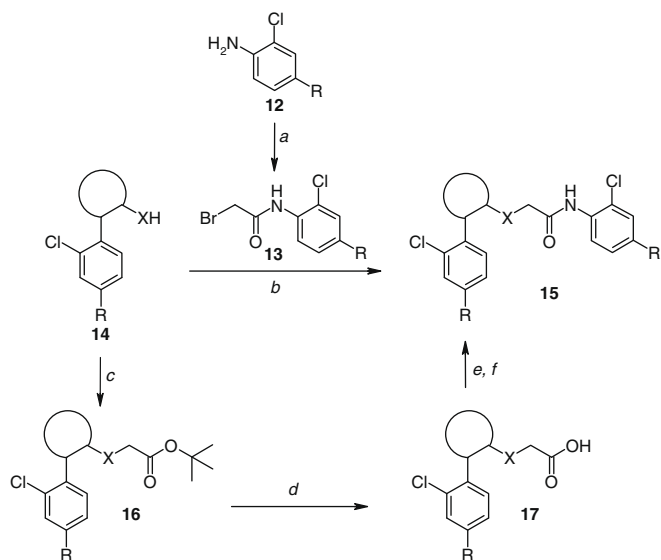
Compound	Linker-X	A	IC ₅₀ ^a (nM) ¹⁵	
			WT	K103N/Y181C
6		OCH ₂ CO ₂ H	1.9	22
7		CH ₂ CO ₂ H	2.4	48
8		OCH ₂ CO ₂ H	15	785
9		OCH ₂ CO ₂ H	272	3272
10		CH ₂ CO ₂ H	18	592
11		CH ₂ CO ₂ H	177	1390

^a IC₅₀ values are the mean of at least two independent experiments.

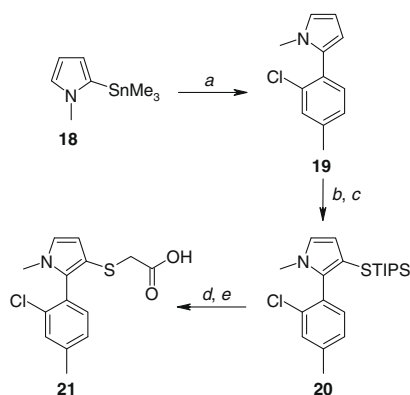
erence, we then evaluated the effect of introducing a phenyl linker and observed a good IC₅₀ against the WT for thiophenyl **10**. However, phenylether **11** suffered from significant loss of potency, indicating a preference for a sulfur over an oxygen as the connecting atom. The erosion of potency against the WT-RT and the drastic loss of activity against the DM-RT observed for all of these linkers suggest that an important electronic contribution is provided by the tetrazole which might additionally be interacting with the surrounding residues in the binding pocket.

Being now aware of the apparent electronic contribution of the tetrazole in the binding of the inhibitors with the RT, we then turned our attention to different five-membered heterocyclic linkers. The synthetic route that we designed to access these inhibitors is based on a previously reported sequence utilized for the preparation of the tetrazolyl inhibitors.¹¹ As illustrated in Scheme 1, two approaches efficiently lead to the desired compounds. The first approach involves the preparation of a bromoacetanilide fragment **13** from the corresponding aniline **12**. This compound is then coupled with a thio or hydroxy aryl heterocycle **14**, directly giving the desired compound **15**. Alternatively, the acetate can be installed first onto **14**, leading to the *tert*-butyl acetate **16**. Removal of the *tert*-butyl group under standard conditions followed by amide bond formation then provides the final product **15**.

The synthesis of compound **15** where the linker is a triazole (compound **28**), a pyrazole (compounds **29**, **30**, **31**, **32**, **33**, and **40**), an imidazole (compounds **35** and **36**), a thiadiazole (compound **37**) or a thiazole (compound **38**) has been described in an earlier report.¹⁰ For the introduction of a pyrrolyl linker into fragment **17**, the synthesis commences with the Stille coupling between stannyl pyrrole **18** and 3-chloro-4-iodotoluene, furnishing the 2-arylpyrrole **19** (Scheme 2). Bromination of **19** followed by lithium-halogen exchange and trapping with TIPS-disulfide then provides the protected thiopyrrole **20**. Removal of the protecting



Scheme 1. Synthetic routes to compound **15**: (a) aniline **12**, bromoacetyl chloride (1.1 equiv), triethylamine (1.1 equiv), CH_2Cl_2 , rt, o.n. (80–100%); (b) fragment **14**, bromoacetamide **13** (1.0 equiv), K_2CO_3 (1.2 equiv), DMF, rt, 2 h (80–100%); (c) fragment **14**, *tert*-butyl bromoacetate (1.1 equiv), K_2CO_3 (1.5 equiv), DMF, rt, o.n. (100%); (d) $\text{CF}_3\text{CO}_2\text{H}$ (10 equiv), CH_2Cl_2 , rt, o.n. (90–100%); (e) ClCOCOCI (1.1 equiv), DMF (0.1 equiv), CH_2Cl_2 , rt, 1.5 h; (f) aniline **12** (1.1 equiv), pyridine (2.0 equiv), CH_2Cl_2 , rt, 4 h, 70–80% (2 steps).

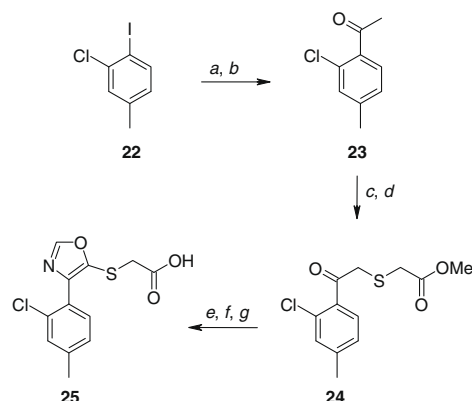


Scheme 2. Synthetic sequence to fragment **21**: (a) 3-chloro-4-iodotoluene (0.9 equiv), $\text{Cl}_2\text{Pd}(\text{PPh}_3)_2$ (0.05 equiv), toluene, 110 °C, o.n. (22%, unoptimized); (b) PBr_3 (0.1 equiv), NBS (1 equiv), THF, –78 °C, 1 h then rt, 3 h (83%); (c) *n*-BuLi (1.0 equiv), TMEDA (1.0 equiv), THF, –78 °C, 1 h then TIPS-S-S-TIPS (1.0 equiv), –78 °C to rt, 2 h (35%, unoptimized); (d) ethyl bromoacetate (2.5 equiv), toluene/DMF (1:1), 0 °C then TBAF (2.5 equiv in toluene), 0.5 h (88%); (e) 1.0 N aq. LiOH (1.5 equiv), THF/MeOH (3:1), 0 °C (100%).

group in the presence of ethyl bromoacetate followed by saponification gives fragment **21**. This pyrrolyl intermediate is finally converted into inhibitor **34** according to [Scheme 1](#).

For the introduction of an oxazole into structure **17**, we started with a Heck reaction between 3-chloro-4-iodotoluene **22** and butyl vinyl ether to provide, after treatment under acidic conditions, ketone **23** ([Scheme 3](#)). This ketone was then brominated and treated with methyl thioglycolate in the presence of base to give **24**. This sulfide was then subjected to bromination prior to undergoing condensation with formamide, and saponification, affording the desired thio-oxazolyl acetic acid **25**. This fragment was finally converted into inhibitor **39** under conditions reported in [Scheme 1](#).

To begin our SAR studies, we first prepared reference compound **26** where the eastern biphenyl aniline is replaced by a simple 2-chloro aniline ([Table 2](#)). The loss of potency associated with this

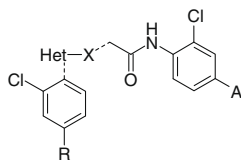


Scheme 3. Synthetic sequence to fragment **25**: (a) Butyl vinyl ether (1.2 equiv), triethylamine (1.2 equiv), $\text{Pd}(\text{OAc})_2$ (0.2 equiv), dppp (0.2 equiv), DMF, 80 °C, 5 h; (b) HCl (4 N in dioxane), dioxane/water (1:1), rt, 1 h (52%, 2 steps); (c) Br_2 (1.1 equiv), dioxane, rt, 1 h (73%); (d) methyl thioglycolate (1.1 equiv), triethylamine (1.1 equiv), CH_2Cl_2 , rt, 1 h (99%); (e) Br_2 (1.0 equiv), AcOH, rt, 0.5 h; (f) formamide (20 equiv), 150 °C, 1 h (39%, 2 steps, unoptimized); (g) 1.0 N aq. NaOH (1.5 equiv), DMSO, rt, 1 h (97%).

modification indicates that substitution *para* to the aniline provides superior potency against the DM-RT. In addition, the potency against the DM-RT could be enhanced by replacing the methyl group in **7** by a larger *tert*-butyl fragment, as exemplified by compound **27**. To evaluate the importance of the nitrogen atoms at position 3 and 4 in compound **7**, we then prepared triazole **28** and pyrazole **29**. Interestingly, removing the nitrogen atom at position 4 (tetrazole numbering) had no detectable impact on the IC_{50} against the WT-RT (triazole **28**). However, proceeding further with the removal of N3 (tetrazole numbering) led to a 4-fold reduction of potency against the WT-RT (pyrazole **29**). In both cases, a drastic loss of potency against the DM-RT was observed.¹⁶ Substitution at position 4 was clearly not tolerated, as illustrated by compound **30**, which was completely inactive against both RTs. The pyrazolyloxy **31** was found to be slightly less potent than the thio analogue **29**, but yet tolerated by the WT-RT. This is in clear contrast to the drastic shift that we observed when going from the thioaryl **10** to the phenoxy **11**. The two isomeric pyrazoles **32** and **33** demonstrate that substitution is only tolerated at the position adjacent to the aryl group. Additionally, pyrrole **34** was more than 500-times less potent than the structurally similar pyrazole **32**, indicating a preference for a nitrogen at position 5 (pyrrole numbering). The above modifications allow us to conclude that a nitrogen atom is preferred over a CH at position 3 and 4 of the heterocyclic linker. Secondly, it appears that substitution is permitted exclusively at position 2.

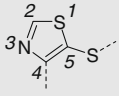
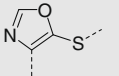
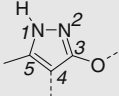
Being now educated on the tolerance of the molecule towards substitution and deletion of nitrogen atoms, we next prepared the imidazole **35** in accordance with the above observations. In the event, excellent potency against the WT-RT was observed for this inhibitor, associated with modest activity against the DM-RT. The 4-methylimidazole **36** was found to be completely inactive against the DM-RT, confirming the observation that substitution at position 3 of the heterocycle is not tolerated. Thiadiazole **37**, which possesses heteroatoms at positions 2, 3 and 4 (tetrazole numbering) proved to be the most potent tetrazole replacement, with a very good IC_{50} against the WT-RT and only a 2-fold loss of activity against the DM-RT. Unfortunately, the low metabolic stability associated with this compound hampered further efforts involving this heterocyclic linker. Replacing one nitrogen atom with carbon in **37** led to thiazole **38** which suffered from modest potency against both RTs, indicating once again a preference for a nitrogen atom at position 3 (tetrazole numbering). The negative

Table 2
Evaluation of heterocyclic linkers



Compound	Het-X	R	A	IC ₅₀ ^a (nM) ¹⁵	
				WT	K103N/Y181C
7		Me	Ph-4-CH ₂ CO ₂ H	2.3	48
26		Me	H	8.8	809
27		<i>t</i> -Bu	Ph-4-CH ₂ CO ₂ H	7.7	28
28		Me	Ph-4-CH ₂ CO ₂ H	2.4	730
29		Me	Ph-4-CH ₂ CO ₂ H	7.9	420
30		Me	Ph-4-CH ₂ CO ₂ H	>10,000	>10,000
31		Me	Ph-4-CH ₂ CO ₂ H	18	770
32		Me	Ph-4-CH ₂ CO ₂ H	1.9	178
33		Me	Ph-4-CH ₂ CO ₂ H	n.d. ^b	6480
34		Me	Ph-4-OCH ₂ CO ₂ H	>1000	2679
35		Me	Ph-4-CH ₂ CO ₂ H	9.5	549
36		Me	H	>1000	>10,000
37		Me	Ph-4-CH ₂ CO ₂ H	2.0	107

Table 2 (continued)

Compound	Het-X	R	A	IC ₅₀ ^a (nM) ¹⁵	
				WT	K103N/Y181C
38		Me	Ph-4-CH ₂ CO ₂ H	200	796
39		Me	Ph-4-CH ₂ CO ₂ H	365	1458
40		t-Bu	Ph-4-CH ₂ CO ₂ H	2089	22

^a IC₅₀ values are the mean of at least two independent experiments.

^b n.d., not determined.

impact on the potency was further exacerbated with the replacement of the sulfur in **38** by an oxygen (oxazole **39**). All of the heterocyclic linkers explored thus far indicate that the tetrazole is not simply acting as an orienting group, but is presumably also interacting with the protein, as supported by the considerable loss of potency observed in all cases with the DM-RT. However, this exercise demonstrates that triazoles, pyrazoles, imidazoles and thiazoles are good tetrazole replacements, providing potent inhibitors of the wild type reverse transcriptase.

We then became interested in the introduction of a H-bond donor in the linker, resulting in the design of pyrazole **40**. To our great delight, an IC₅₀ of 22 nM against the DM-RT was observed for this inhibitor. More fascinating was the significant loss of activity observed against the WT-RT. Intrigued by this reversal of selectivity, we initiated a more detailed SAR study on this pyrazolyl scaffold (Table 3).

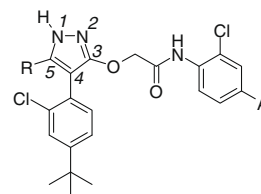
To evaluate the importance of the methyl group at position 5 of the pyrazole, we first prepared the *des*-methyl **41** and observed a significant reduction in the potency against the DM-RT. However, encouraged by the cellular potency obtained against the DM-RT, we pursued our investigation on these NH-pyrazolyl inhibitors. The introduction of our previously reported alkynyl aniline fragment led to an improvement in the cellular potency against the DM-RT, as exemplified by compound **42**. Further advancement was achieved with the introduction of the dimethyl butynoic acid fragment (compound **43**), giving our best EC₅₀ against the DM-RT for this class of compound.

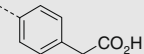
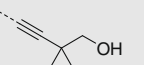
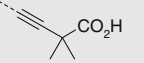
In order to evaluate the relation between the electrostatic properties of the linkers and the potency of the inhibitors, we next calculated the electrostatic potential (ESP) of selected compounds (Fig. 4). As illustrated, tetrazole **7**, triazole **28** and thiazazole **37**, which were all very potent against the WT-RT, all have a strong negative potential localized around the edge of the heterocycle.

Conversely, pyrazoles **29** and thiazole **38**, which had poorer potency against the WT-RT, have a slightly positive ESP. In the case of the pyrazole **40**, which had poor potency against the WT-RT, a strong positive potential localized on the NH is observed. Consequently, it appears that a strong negative ESP near position 3 leads to higher potency against the WT-RT, but not against the DM-RT.

To rationalize the unforeseen loss of potency against the WT-RT observed with the NH-pyrazolyl inhibitors and to gain a deeper understanding on the role of the linker in the binding of the tetrazolyl inhibitors, a molecular model of compound **27** and **40** in the NNRTI binding pocket of the HIV-1 WT and K103N/Y181C DM RTs was generated (Fig. 5).¹⁸ In accordance with our previous studies,^{11,12} the model shows the orthogonality between the tetrazole

Table 3
SAR studies on the oxypyrazole acetanilide series



Compound	R	A	IC ₅₀ ^a (nM) ¹⁵		EC ₅₀ ^a (nM) ¹⁷	
			WT	K103N/Y181C	WT	K103N/Y181C
41	H		>3300	122	4869	444
42	Me		>3330	24	>5000	177
43	Me		2403	38	3884	73

^a IC₅₀ and EC₅₀ values are the mean of at least two independent experiments.

and the directly attached aryl group. Additionally, the carbonyl of the amide is at an optimal distance for a hydrogen bond with the backbone of residue 103. The left hand side aryl group binds in a hydrophobic pocket formed by residues 229, 188 and 181 while the tetrazole rests in close proximity to residue 103. The erosion of potency observed following substitution at position 3 and 4 (tetrazole numbering) can be explained by a steric clash or an unfavorable interaction between the alkyl group and the side chain of residue 103. Additionally, a steric repulsion between the CH₂ group of the acetamide and a 4-methyl group might result in a higher energy bioactive conformation.

In accordance with our initial hypothesis,¹² our studies indicate that the tetrazole can interact with residue 103. In fact, the model suggests a possible (tetrazole)N...H-C_{sp}3 interaction between N3 and N4 of the tetrazole and the γ -H of the side chain of lysine-103.¹⁹ Previous studies have established that the side chain of lysine is one of the best donors in the C-H... π interaction.²⁰ Moreover, this interaction is supported by the electrostatic potential calculated for **7** which places the electronic density on the edge

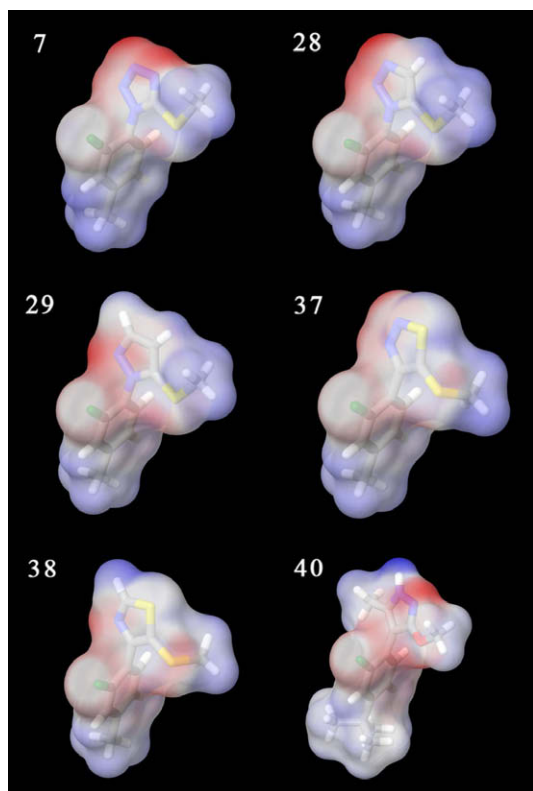


Figure 4. Electrostatic potential (ESP) of selected inhibitors calculated at the HF/6-31G* level of theory. Red represents a negative potential; white represents a neutral potential; blue represents a positive potential.

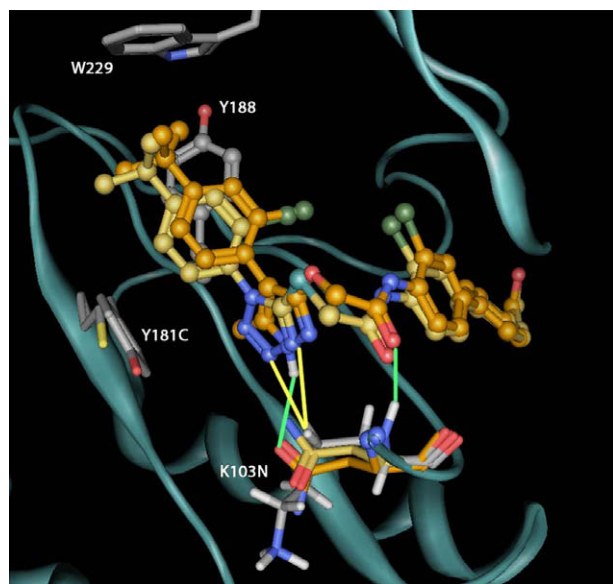


Figure 5. Molecular model of **27** (yellow) and **40** (orange) in the allosteric site of HIV-1 WT and K103N/Y181C RT.

of the heterocycle. In the case of the pyrazole **40**, this interaction would be replaced by an unfavorable (pyrazolyl)N–H.../–H–C_{sp3} contact, resulting in a major loss of potency against the WT-RT. In the case of the 103N mutant, the side chain of the asparagine can accommodate a H-bond donor or H-bond acceptor by rotation of the amide, resulting in a (tetrazole)N...H₂NCO_{103N} for **27** or (pyrazolyl)N–H...O=C_{103N} for **40**. The poor potency observed

against the DM-RT for many heterocyclic linkers would therefore be explained by the lack of an adequate H-bond acceptor.

In conclusion, the role of the tetrazolyl group in the binding of the thiotetrazole acetanilide inhibitors with the HIV-1 reverse transcriptase has been studied through the design of different cyclic and acyclic tetrazole replacements. We have demonstrated that a simple Z alkene is capable of retaining most of the potency against the WT-RT, supporting the hypothesis that the tetrazole partially acts as an orienting scaffold. The exploration of numerous heterocyclic linkers allowed the identification of potent inhibitors of the WT-RT. A complete reversal of selectivity was observed for the NH-pyrazolyl inhibitors, giving excellent potency against the DM-RT associated with a complete loss of activity against the WT-RT. The electrostatic potential study has demonstrated that the tetrazole provides a strong negative potential located at the edge of the heterocycle. Modeling studies of the tetrazolyl and NH-pyrazolyl inhibitors suggested important interactions between the heterocyclic linkers and residue 103, providing a rationale for the potency observed against both RTs.

Acknowledgments

We are grateful to colleagues at Boehringer Ingelheim (Canada) Ltd. for analytical support, biological evaluation and valuable help during manuscript preparation.

References and notes

1. AIDS epidemic update, UNAIDS, World health organization, December 2007, <http://www.unaids.org>.
2. For a review on recent developments in the treatment of AIDS, see: Armbruster, C. *Anti-Infective Agents Med. Chem.* **2008**, *7*, 201.
3. For an excellent review on the HIV-RT, see: Castro, H. C.; Loureiro, N. I. V.; Pujol-Luz, M.; Souza, A. M. T.; Albuquerque, M. G.; Santos, D. O.; Cabral, L. M.; Frugulhetti, I. C.; Rodrigues, C. R. *Curr. Med. Chem.* **2006**, *13*, 313.
4. For a recent reference on the mechanism of NNRTIs, see: Sluis-Cremer, N.; Tachedjian, G. *Virus Res.* **2008**, *134*, 147.
5. For excellent reviews on the current status of NNRTIs, see: (a) Martins, S.; Ramos, M. J.; Fernandes, P. A. *Curr. Med. Chem.* **2008**, *15*, 1083; (b) Sweeney, Z. K.; Klumpp, K. *Curr. Opin. Drug Discov. Dev.* **2008**, *11*, 458; (c) Sahlberg, C.; Zhou, X.-X. *Anti-Infective Agents Med. Chem.* **2008**, *7*, 101.
6. Simoneau, B.; Thavonekham, B.; Landry, S.; O'Meara, J.; Yoakim, C.; Faucher, A. -M. 2004 WO 2004/050643.
7. (a) Muraglia, E.; Kinzel, O. D.; Laufer, R.; Miller, M. D.; Moyer, G.; Munshi, V.; Orvieto, F.; Palumbi, M. C.; Pescatore, G.; Rowley, M.; Williams, P. D.; Summa, V. *Bioorg. Med. Chem. Lett.* **2006**, *16*, 2748; (b) Shaw-Reid, C. A.; Miller, M. D.; Hazuda, D. J.; Ferrer, M.; Sur, S. M.; Summa, V.; Lyle, T. A.; Kinzel, O.; Pescatore, G.; Muraglia, E.; Orvieto, F.; Williams, P. D. 2005 WO 2005/115147.
8. For a review on RT mutations, see: Martinez-Picado, J.; Martínez, M. A. *Virus Res.* **2008**, *134*, 104.
9. For general reviews on resistance to current HIV therapies, see: (a) Shafer, R. W.; Shapiro, J. M. *AIDS Rev.* **2008**, *10*, 67; (b) Perno, C.-F.; Moyle, G.; Tsoukas, C.; Ratanasuwana, W.; Gatell, J.; Schechter, M. J. *Med. Virol.* **2008**, *80*, 565.
10. DeRoy, P.; Faucher, A. -M.; Gagnon, A.; Landry, S.; Morin, S.; O'Meara, J.; Simoneau, B.; Thavonekham, B.; Yoakim, C. 2005 WO 2005/118575.
11. Gagnon, A.; Amad, M. H.; Bonneau, P. R.; Coulombe, R.; DeRoy, P. L.; Doyon, L.; Duan, J.; Garneau, M.; Guse, I.; Jakalian, A.; Jolicœur, E.; Landry, S.; Malenfant, E.; Simoneau, B.; Yoakim, C. *Bioorg. Med. Chem. Lett.* **2007**, *17*, 4437.
12. O'Meara, J. A.; Jakalian, A.; LaPlante, S.; Bonneau, P. R.; Coulombe, R.; Faucher, A.-M.; Guse, I.; Landry, S.; Racine, J.; Simoneau, B.; Thavonekham, B.; Yoakim, C. *Bioorg. Med. Chem. Lett.* **2007**, *17*, 3362.
13. (a) Girardet, J.-L.; Zhang, Z.; Hamatake, R.; Hernandez, M. A. De la Rosa; Gunic, E.; Hong, Z.; Kim, H.; Koh, Y. -h.; Nilar, S.; Shaw, S.; Yao, N. 2004 WO 2004/030611.; (b) Wang, Z.; Wu, B.; Kuhen, K. L.; Bursulaya, B.; Nguyen, T. N.; Nguyen, D. G.; He, Y. *Bioorg. Med. Chem. Lett.* **2006**, *16*, 4174; De La (c) Rosa, M.; Kim, H. W.; Gunic, E.; Jenket, C.; Boyle, U.; Koh, Y.-h.; Korboukh, I.; Allan, M.; Zhang, W.; Chen, H.; Xu, W.; Nilar, S.; Yao, N.; Hamatake, R.; Lang, S. A.; Hong, Z.; Zhang, Z.; Girardet, J.-L. *Bioorg. Med. Chem. Lett.* **2006**, *16*, 4444; (d) Zhang, Z.; Xu, W.; Koh, Y.-H.; Shim, J. H.; Girardet, J.-L.; Yeh, L.-T.; Hamatake, R. K.; Hong, Z. *Antimicrob. Agents Chemother.* **2007**, *51*, 429.
14. Zhan, P.; Liu, X.; Cao, Y.; Wang, Y.; Pannecouque, C.; De Clercq, E. *Bioorg. Med. Chem. Lett.* **2008**, *18*, 5368.
15. IC₅₀ values for WT and mutant RTs were obtained from a scintillation proximity assay using poly rC/biotin-dG₁₅ and ³H-dGTP at 37 °C.
16. For compound **28**, a 28-fold and a 5-fold loss of potency was observed, respectively, for K103N and Y181C single mutants, suggesting that the loss of

- potency against the K103N/Y181C double mutant is mainly due to the 103 mutation.
17. For EC₅₀ determinations, C8166 cells were acutely infected (MOI 0.001) and incubated with inhibitors for 3 days at 37 °C. Viral replication was assessed by p24 ELISA of the culture supernatants.
 18. Models of **27** and **40** were generated by modifying an unpublished in-house X-ray structure of a related compound. Mutations K103N and Y181C were performed in silico based on pdb 1FKP and 1UWB, respectively. Energy minimization was performed on the binding site for each inhibitor/mutation complex.
 19. For studies on related C–H...O=C interactions, see: (a) Tóth, G.; Bowers, S. G.; Truong, A. P.; Probst, G. *Curr. Pharm. Design* **2007**, *13*, 3476; (b) Panigrahi, S. K.; Desiraju, G. R. *Proteins: Structure, Function, and Bioinformatics* **2007**, *67*, 128.
 20. Brandl, M.; Weiss, M. S.; Jabs, A.; Sühnel, J.; Hilgenfeld, R. *J. Mol. Biol.* **2001**, *307*, 357.